DOI: 10.13009/EUCASS2019-507

Application of hybrid numerical schemes in prediction of high-speed laminar-turbulent transition

*Ivan V. Egorov * and Can Nguyen***
**Central Aerohydrodynamic Institute*
1 *Zhukovsky st., Zhukovsky, Moscow region, Russia*, *ivan.egorov@tsagi.ru*
***PhD student, Moscow Institute of Physics and Technology*
9 Institutsky pereulok, Dolgoprudny, Moscow region, Russia

Abstract
The problem of laminar-turbulent transition (LTT) in hypersonic boundary-layer flows is one of the main still unsolved problems of high-speed aerodynamics. LTT leads to a substantial increase of the surface heating and aerodynamic drag of hypersonic vehicles and, thereby as well as affects the efficiency of propulsion system and control surfaces. In this paper we discuss our DNS of a transitional flow over a flat plate at the freestream Mach number 3 and high unit Reynolds numbers. Hybrid difference schemes allow increasing accuracy of numerical data in comparison with fully monotone difference schemes on the same numerical grid.

1. Introduction

The problem of laminar-turbulent transition (LTT) in hypersonic boundary-layer flows is one of the main still unsolved problems of high-speed aerodynamics. LTT leads to a substantial increase of the surface heating and aerodynamic drag of hypersonic vehicles and, thereby as well as affects the efficiency of propulsion system and control surfaces.
A holistic computation of the all LTT stages is possible only using direct numerical simulations (DNS), where the full unsteady three-dimensional (3D) Navier–Stokes equations are solved without any restriction on the mean (unperturbed laminar) flow and disturbance amplitudes. In addition, as opposed to physical experiments, DNS gives full information about 3D disturbance field, which enables to identify and study in detail different LTT mechanisms. The modern methods of parallel computations and rapid developments of multi-processor supercomputers make it feasible to conduct such numerical experiments for hypersonic boundary layers for simple configurations such as a flat plate and a cone at zero angle of attack [1]. Further progress in computational hardware will allow us to handle more and more complicated and practical configurations. At the same time it is necessary to use difference schemes with minimum dissipative properties that don't lead to numerical instability in order to increase effectiveness of numerical simulation. Such difference schemes can be hybrid schemes, which are an approximation of convective terms in Navier-Stokes equations with use of central difference schemes and monotone schemes with weights. This talk will demonstrate that use of hybrid difference schemes allow increasing accuracy of numerical data in comparison with fully monotone difference schemes on the same numerical grid.
In particular, we discuss our DNS of a transitional flow over a flat plate at the freestream Mach number 3 and high unit Reynolds numbers. The flow parameters are the same as at [2]. It is shown that depending on different numerical schemes the behavior depended variables can evolved in quantitatively different ways. Future efforts related to the LTT simulation as well as other issues on practical applications of DNS will be also thoroughly addressed.

2. The problem statement

Scheme of the problem under consideration is shown in Figure 1 and Figure 2. Generator of unsteady disturbances is located on the plate surface in the vicinity of its sharp leading edge. In accordance with [2], development of the first

DOI: 10.13009/EUCASS2019-507

mode in boundary layer on the plate, streamlined by supersonic flow at Mach number 3, unit Reynolds $\mathrm{Re}_1 = 2.181\times10^6\, m^{-1}$ and free stream temperature $T_\infty = 103.6\,\mathrm{K}$. Gas is assumed to be perfect with adiabatic exponent 1.4 and Prandtl number 0.72. Viscosity is calculated using Sutherland formula with 110.4 K. The plate surface is adiabatic $(\partial T/\partial \mathbf{n})_w = 0$.

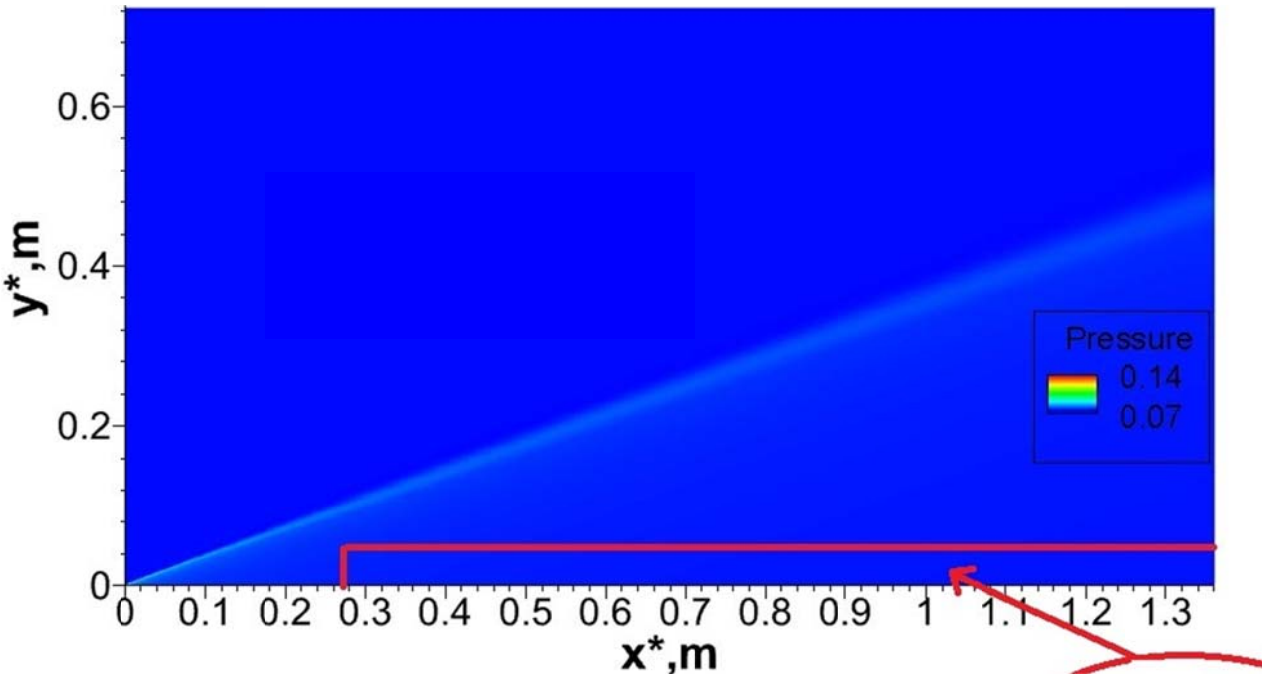

Figure 1: Pressure field obtained in calculations

On the plate, in the *x* range: $x_1 < x < x_2$ ($x_1 = 0.394\ m$ and $x_2 = 0.452\ m$, $x_2 - x_1 = \lambda_x$), normal velocity component is specified using formula from work [2]:

$$v(x, y=0, t) = A(t)v_p(x_p)\cos(\beta z)\cos(-\omega t)$$

where

$$v_p = \begin{cases} 1.5^4(1+x_p)^3(3(1+x_p)^2 - 7(1+x_p)+4), & -1 \le x_p \le 0 \\ -1.5^4(1-x_p)^3(3(1-x_p)^2 - 7(1-x_p)+4), & 0 \le x_p \le 1 \end{cases}, \quad x_p = \frac{2x-(x_2+x_1)}{x_2-x_1}$$

$$A(t) = 0.003\begin{cases} 0 & , \quad t<0 \\ 0.1^{((T-t)/(0.9T))^2} & , \quad 0 \le t \le T \\ 1 & , \quad t>T \end{cases}$$

Here $T = 2\pi/\omega$, $A(t)$ - amplitude, ϕ - initial phase. Disturbance frequency is equal to 6.36 kHz, transverse wave number $\beta^* = 211.52\ \mathrm{m}^{-1}$, initial disturbance amplitude 0.3%.

DOI: 10.13009/EUCASS2019-507

In Figure 2 three dimensional grid is shown in cut sub-domain, which is used for all calculations, considered in this work. In physical space the grid has about 3.3 million nodes. On the left ($x_0 = 0.258\ m$ from the leading edge of the plate) and upper boundaries flow parameters are specified from two-dimensional calculations on whole computational domain. Outflow boundary is approximately located at $18.05\lambda_x$. Height of the computational domain is chosen as $y_H \approx 0.043\ m$, that is approximately 6.5 of local boundary layer thicknesses on the outflow boundary. Spanwise wave number $\beta = 211.52\ m^{-1}$ т.е. $z_w = \lambda_z = 2\pi / \beta = 0.03$ m .

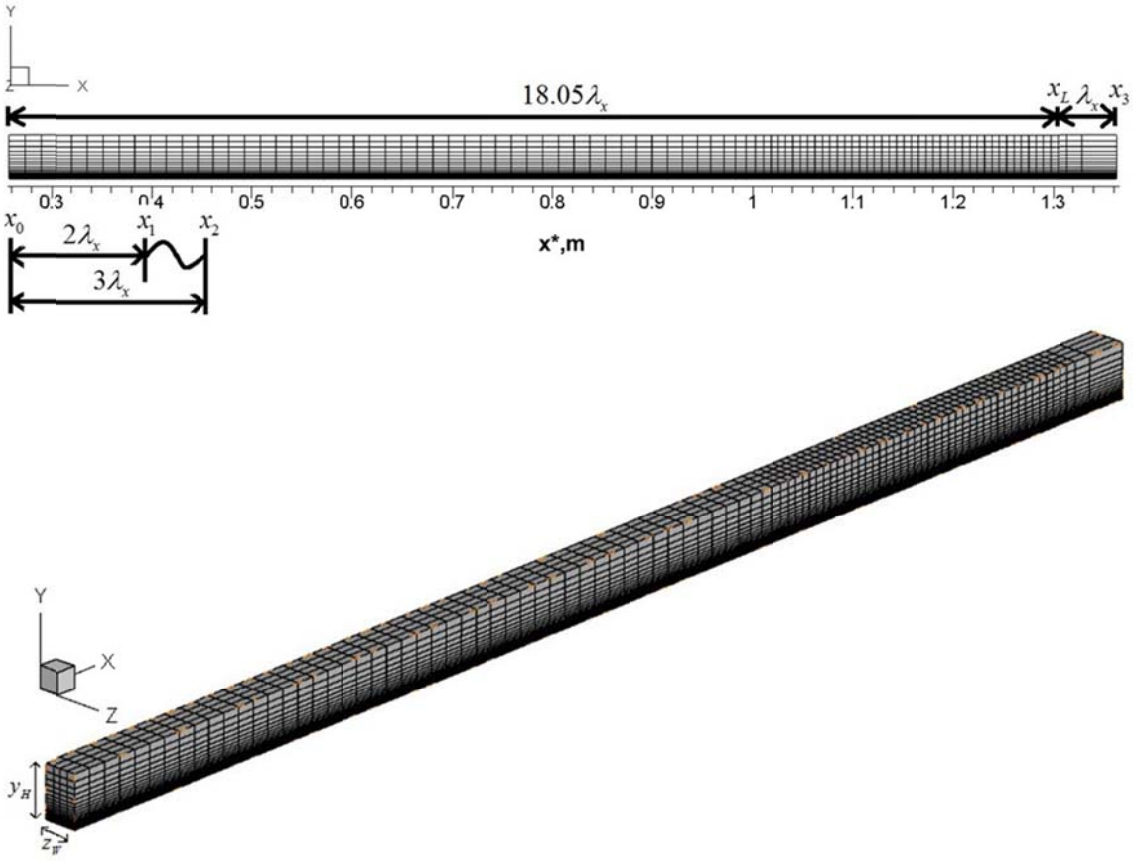

Figure 2: Numerical grid structure

3. Solution technique

Calculations are carried out using HSFlow code[3-5], in which system of three-dimensional unsteady Navier-Stokes equations is solved for perfect gas with constant adiabatic exponent and Prandtl number. For calculations of flow over the plate implicit conservative TVD scheme of the second order of approximation in time and space for dissipative terms is used. Convective terms are approximated using WENO scheme of the third order of approximation.

This scheme is not high order approximation scheme, its numerical dissipation can be reduced using rather fine grid. This allows making reliables imulation of such unsteady processes as receptivity and instability of supersonic boundary layers [3], nonlinear development of disturbances in boundary layer on the plate [5] and in zone of laminar separation on compression corner [4].

Navier-Stokes equations are integrated in dimensionless variables: $x = X / L$, $y = Y / L$, $z = Z / L$, $u' = u / u_\infty$, $v' = v / u_\infty$, $w' = w / u_\infty$, $t' = t\, u_\infty / L$, $\rho' = \rho / \rho_\infty$, $p' = p / \left(\rho_\infty u_\infty^2\right)$, $T' = T / T_\infty$, $\mu' = \mu / \mu_\infty$. Let us consider sub-domain, where strong discontinuities are absent, such as shock waves (Figure 1, red line). In order to increase accuracy in this sub-domain hybrid difference scheme can be used with minimal dissipation. In this caseapproximation of convective vector in half-integer node is:

$$\vec{E}_{i+\frac{1}{2}} = \frac{1}{2}\left[\vec{E}(Q_L) + \vec{E}(Q_R) - \Phi \times \overline{B}_{LR}\overline{\Lambda}(\varphi(\lambda_{LRi}))\overline{B}_{LR}^{-1}(\vec{Q}_R - \vec{Q}_L)\right]$$

DOI: 10.13009/EUCASS2019-507

Here $\Phi = \begin{cases} \max(\Phi_0, \Psi) \\ 1 \end{cases}$

Φ_0 - parameter of difference scheme, Ψ - Jameson function from [6]:

$$\Psi = \frac{(\mathrm{div}V)^2}{(\mathrm{div}V)^2 + (\mathrm{rotV})^2 + \varepsilon}, \quad \varepsilon = 10^{-20}$$

ε is positive real number to prevent numerical divergence in regions where $\mathrm{div}\vec{V}$ and $\mathrm{rot}\vec{V}$ are close to zero. Value of Ψ is between 0 and 1.

In buffer zone parameter Φ tends to 1 in order to suppress of perturbations of dependent variables, difference scheme is fully monotone.

For illustration in Figure 3 distribution of Ψ function for 2D steady field without disturbances is shown. In solution of unsteady problem in sub-domain with forced disturbances values of this function are fixed. In transverse direction z function Ψ isn't changed.

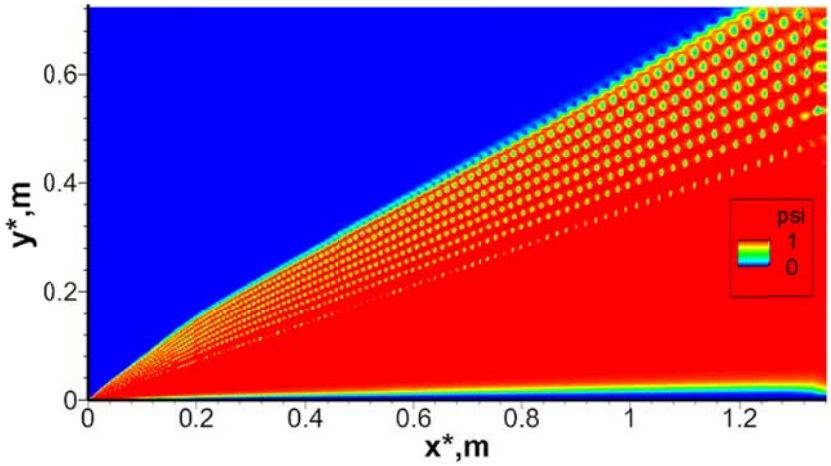

Figure 3: Field of Jameson function

Figure 4 illustrates behaviour of longitudinal velocity $u(y)$ and function profiles $\Psi(y)$. Value of $\Psi(y)$ is equal to zero in boundary layer and tends to 1 outside boundary layer.

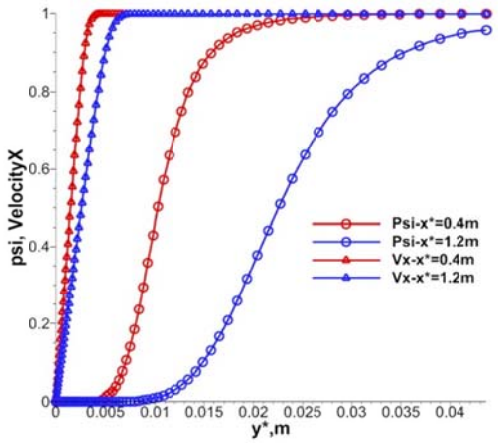

Figure 4: Profiles of longitudinal velocity component and function $\Psi(y)$ in two sections

DOI: 10.13009/EUCASS2019-507

4. Results of numerical simulation

Results of calculations with forced disturbances show that at $\Phi_0 \le 0.25$ hybrid numerical scheme works unstable. During the integration in time nonphysical oscillations appear. At $\Phi_0 \ge 0.3$ nonphysical oscillations are not observed. Further calculations are carried out for 3 cases: monotone difference scheme and hybrid scheme ($\Phi_0 = 0.3$, 0.4).

Integration in time is carried out until the moment of quasi-periodic flow regime achievement, which is attained approximately after 2500 time steps after start of disturbance generator These data are illustrated in Figure 5, where evolution of residual in Newton method after the first iteration for nonlinearity is shown. All solution averaging procedures are fulfilled using integer number of periods for quasi-periodic regime.

Let us consider structure of Q-criterion: Q > 0, where Q is defined by formulas:

$$Q = \frac{1}{2}\left[|\bar{\Omega}|^2 - |\bar{S}|^2\right]$$

$$\bar{S} = \frac{1}{2}\left[\nabla\vec{V} + (\nabla\vec{V})^T\right], \bar{\Omega} = \frac{1}{2}\left[\nabla\vec{V} - (\nabla\vec{V})^T\right]$$

Visualization of the vortex structure of flow in boundary layer for numerical schemes under consideration is shown in Figure 6. Data obtained in the calculations on linear regime are compared with results of work [2] in Figure 7.

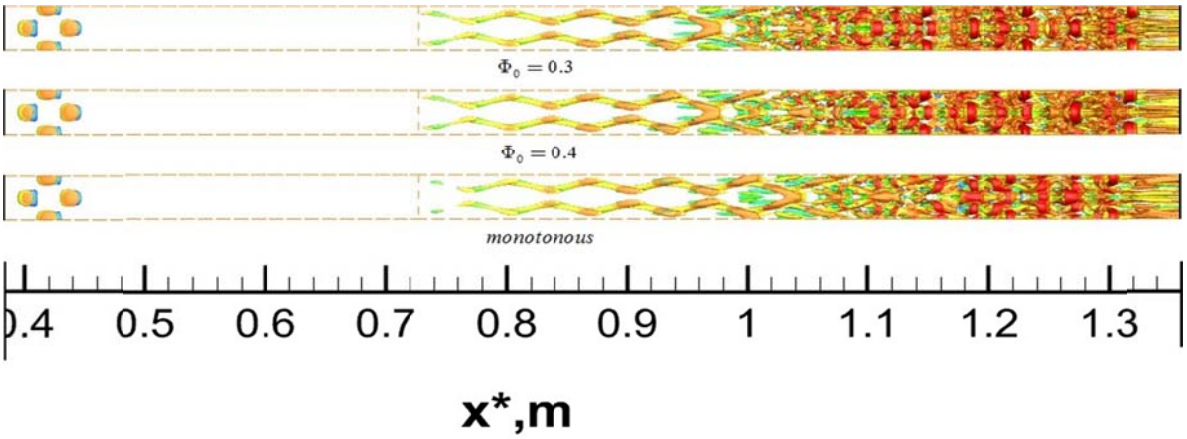

Figure. 6: Q-criterion (Q=15). Top view

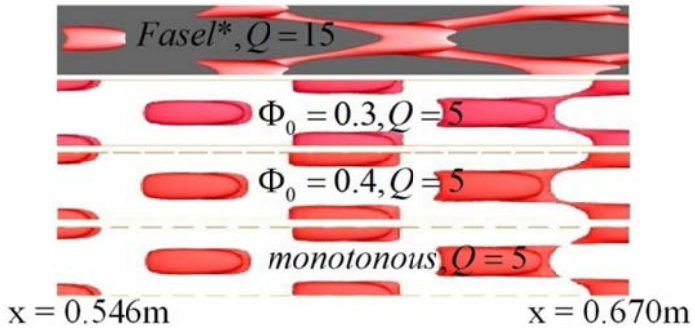

Figure 7: Q-criterion from x=0.546m to x=0.670m

According to data in Figure 7 agreement on linear regime is satisfactory. Maximum pulsation amplitude of longitudinal velocity is shown in Figure 8. Calculations are carried out during time $\Delta t \approx 2T_{forcing}$. These data show

DOI: 10.13009/EUCASS2019-507

good agreement of present results with results of work [2]. From Figure 8 it is seen that hybrid schemes give higher amplitude of longitudinal velocity pulsations, that monotone scheme.

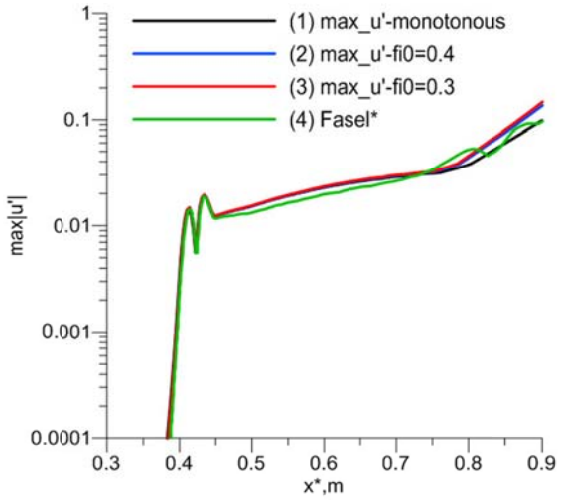

Figure 8: Amplitude of longitudinal velocity pulsations

Using results of numerical simulation complex wave number is calculated using following formulas:

$$\alpha_i = -\frac{d}{dx}[\ln(A(x)|_{crit})]$$

$$\begin{aligned}\Omega' = \Omega(y).\exp[\mathrm{i}(\alpha\,\mathrm{x} + \beta z - \omega t)],\ \alpha = \alpha_r + i\alpha_i \\ = \Omega(y).e^{-\alpha_i x}.\exp[i(\alpha_r\,\mathrm{x} + \beta z - \omega t)] \\ = A(x).\exp[i(\alpha_r\,\mathrm{x} + \beta z - \omega t)],\ \ A(x) = \Omega(y).e^{-\alpha_i x}\end{aligned}$$

In our calculations α_i is calculated for the case of the maximum amplitude of longitudinal velocity in normal to wall direction.

According to data in Figure 9 onset of nonlinear breakdown of disturbances is delayed when relatively coarse numerical grid and described schemes are used in comparison with results of work [2]. Monotone scheme gives the largest delay (the longest distance of linear development of disturbances) in comparison with hybrid schemes.

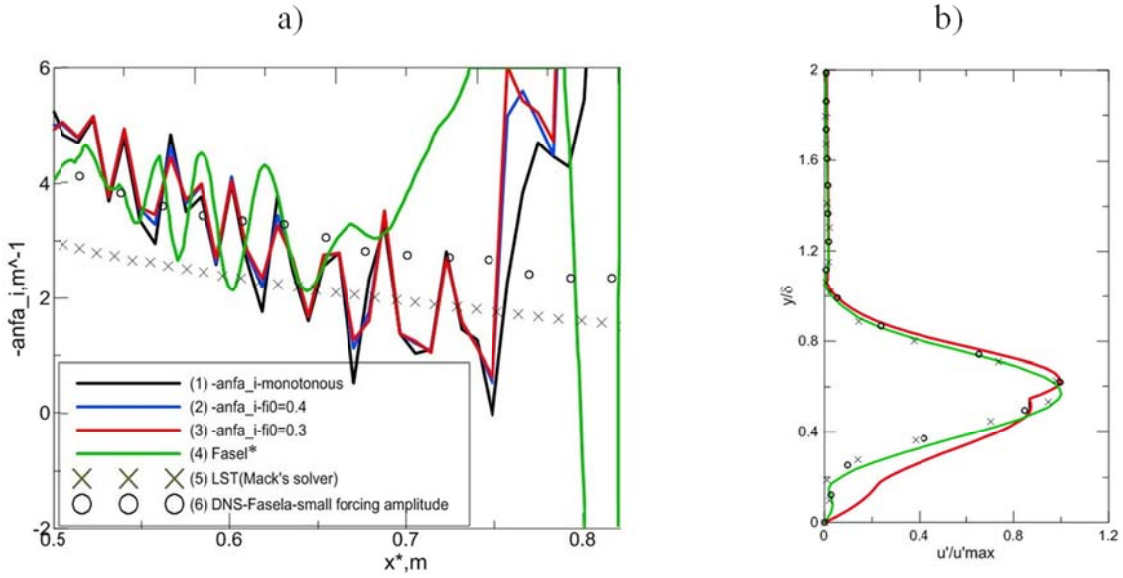

Figure 9: Development of oblique nonlinear wave: a) increment of longitudinal enhancement ; b) normal amplitude of longitudinal disturbance velocity in section x=0.65 m

DOI: 10.13009/EUCASS2019-507

Let us consider nonlinear regime of disturbance development, appearance of which gives indirect evidence of laminar-turbulent transition onset. The moment of nonlinear interactions appearance can be seen in pictures of *Q*-criterion, which reveal enhanced "spindle-shaped" paths (Figure 10). Region of considerable nonlinear effects appearance, mentioned in this work, is located downstream in comparison with the work [2]. It is seen that in region $X > 0.87$ m nonlinear breakdown of large-scale vortex disturbance begins. In boundary layer small-scale structures appear, which are characteristic for developed turbulence. Their shape and intensity agree well with results of work [2]. Application of hybrid difference schemes leads to motion of this region upstream, that is illustrated in Figure 11. The best result is observed at $\Phi_0 = 0.3$.

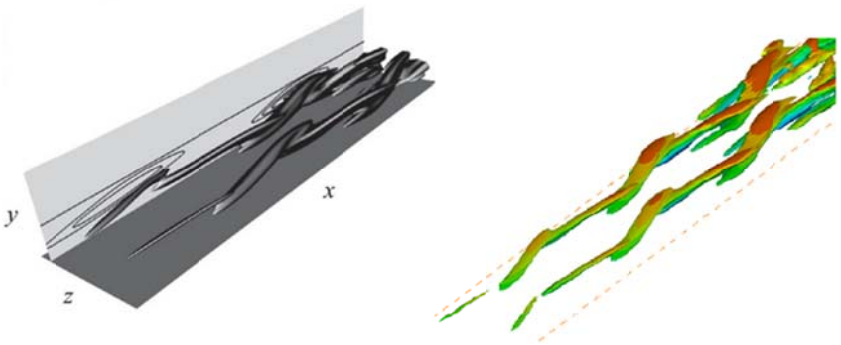

Figure 10: Iso-surface of Q-criterion (Q=100) in the region from x=0.670 m to x=0,798 m of work [2] (left) and in the region from x=0.910 m to x=1,080 m monotone scheme of this work (right)

Vortex flow structures in different sections in coordinate *x* are shown in Figure 12. Delay of the regular structures breakdown in comparison with work [2] can be noted. Peak value of vorticity in this work is also less than in work [2]. Small-scale structures are worse seen, that is governed by use of coarse grid. Results, obtained with use of hybrid scheme $\Phi_0 = 0.3$ give the highest peak value of vorticity; with use of monotone scheme – the least one. Structure of wake in sections *x=const* differs from results of work [2] (see Figure 13). However, application of hybrid scheme allows improving results in comparison with monotone scheme.

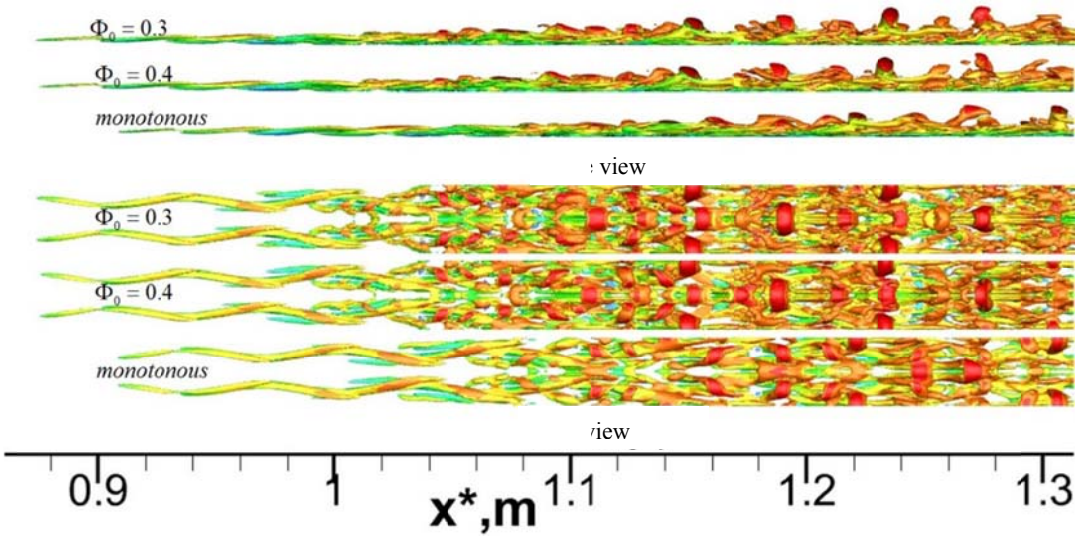

Figure 11: Flow structure with use of Q-criterion (Q=100)

DOI: 10.13009/EUCASS2019-507

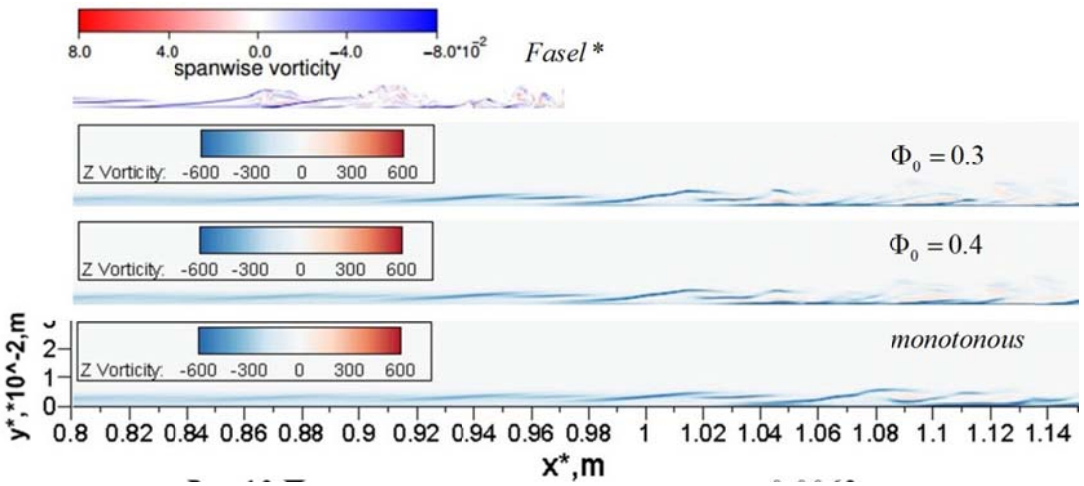

Figure 12: Transverse vortex structure, z=0.0062 m

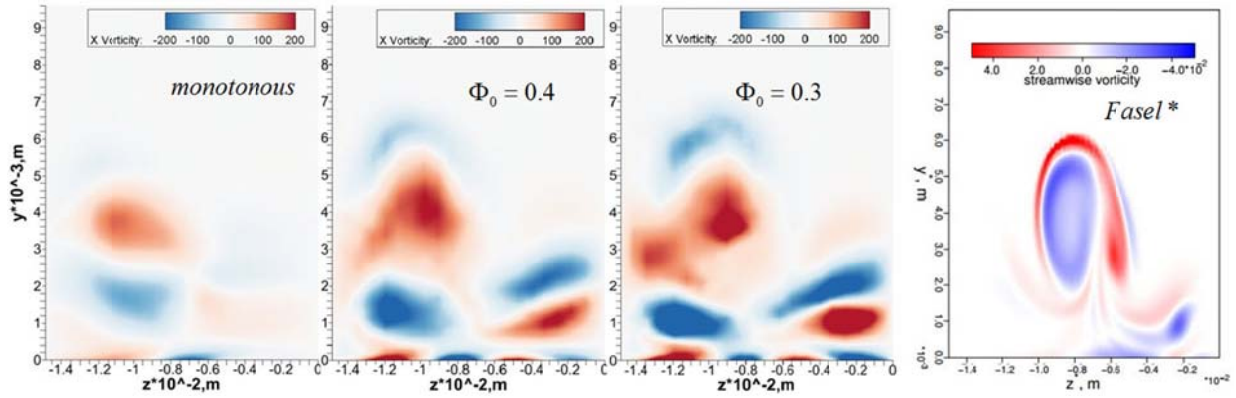

Figure 13: Longitudinal vortex structure, x=1.062 m, [2] — x=0.862 m

Let us consider friction coefficient, which is calculated using formula:

$$C_f = \frac{2\bar{\mu}\frac{\partial \bar{u}}{\partial y}|_{y=0}}{\mathrm{Re}_\infty^L}, \ \mathrm{Re}_{\infty,L} = \frac{U_\infty L}{\nu_\infty}, \ L = 0.7239 \ m$$

here line above a symbol means averaging in time and in spanwise direction in all computational domain using formula:

$$\bar{\phi} = \frac{1}{\lambda_z}\frac{1}{\Delta t}\int_0^{\lambda_z}\int_{t_0}^{t_0+\Delta t}\phi(t,z)dtdz$$

It is shown in Figure 14 that monotone scheme leads to later onset of LTT, and hybrid schemes give result, close to work [2]. At the same time it is seen that difference between results of this work for schemes with $\Phi_0 = 0.3$ and $\Phi_0 = 0.4$ is not significant.

DOI: 10.13009/EUCASS2019-507

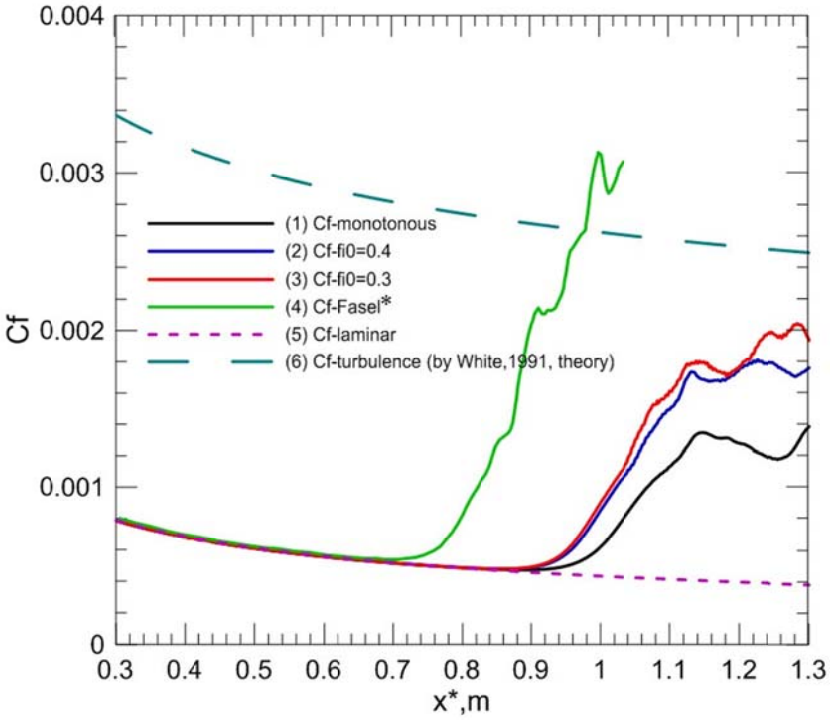

Figure14: Friction coeffcient

For detailed comparison of monotone and hybrid schemes profiles of Favre averaged velocity and temperature profiles in section x=1.25 m is considered (Figure 15).

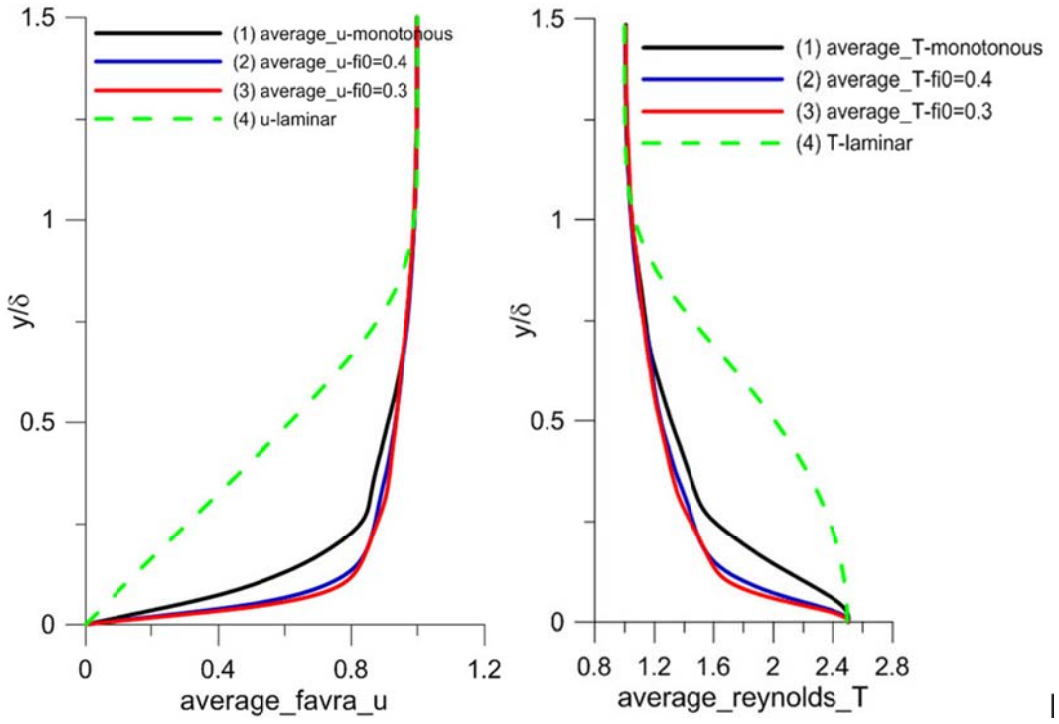

Figure15: Profiles of Favre averaged longitudinal velocity and Reynolds averaged temperature in section

DOI: 10.13009/EUCASS2019-507

Profiles in case of hybrid scheme with $\Phi_0 = 0.3$ come to the wall with higher inclination in comparison with other profiles. This is an indication of higher degree of turbulization in this section in case of hybrid scheme use with the minimum applicable value Φ_0 .

Consider characteristic wall scale of velocity and length, which are given by formulas:

$$u_\tau = \sqrt{\frac{\tau_w}{\rho}},\ l_\tau = \frac{\nu}{u_\tau}$$

Wall (universal) variables are:

$$u^+ = u / u_\tau,\ y^+ = y / l_\tau$$

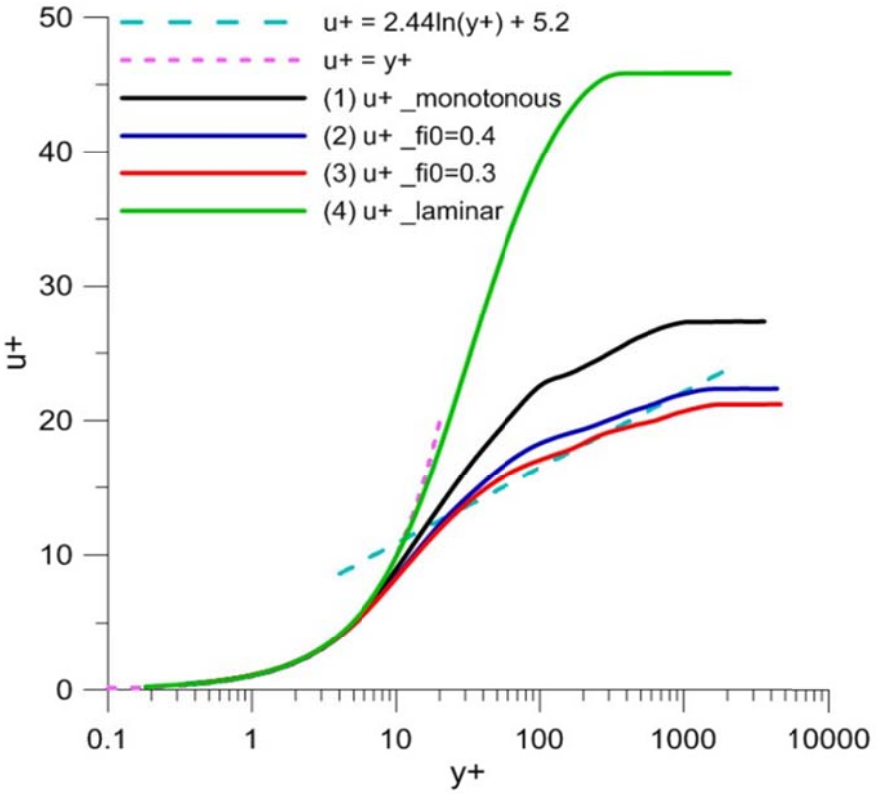

Figure16 : Profile of longitudinal velocity in wall variables (logarithmic scale along axis y^+) in section x=1.25 m

Profiles $u^+\left(y^+\right)$ are given in Figure 16. It is seen that profiles for case of hybrid schemes agree better with logarithmic wall law for developed turbulent boundary layer, $u^+ = 2.44\ln\left(y^+\right) + 5.2$,than in case of monotone scheme.

Conclusions

In this work hybrid numerical method for solution of two-dimensional and three-dimensional Navier-Stokes equations for perfect gas is developed, implemented and tested. Developed non-monotone hybrid scheme allows to control dissipation, depending on parameters of local flow. In particular, monotonizing correction decreases till given threshold level inside boundary layer. Influence of dissipative component of difference scheme on basic characteristics of laminar-turbulent transition in supersonic flow over flat plate is investigated. Test calculaions are

DOI: 10.13009/EUCASS2019-507

carried out using rather coarse grids (about three million nodes), satisfactory results are obtained. In comparison with case of monotone difference scheme, solution with use of hybrid scheme agrees better with data of other works, in which different numerical methods and finer grids with up to 80 million nodes are used.

Acknowledgment

This work was supported by the Russian Scientific Foundation (project 19-19-00470) fulfilment of computational investigations and analysis of results) and RFBR (project 17-08-00969, the algorithm and programs for numerical simulation development).

References

[1] Zhong X. and Wang X. 2012. Direct Numerical Simulation on the Receptivity, Instability, and Transition of Hypersonic Boundary Layers. *Annu. Rev. Fluid Mech.*, **44**. 527-561.

[2] Mayer C. S. J., von Terzi D. A., Fasel H. F. 2009. DNS of complete transition to turbulence via oblique breakdown at Mach 3: Part. ii . *AIAA Paper* 2009-3558.

[3] Egorov I.V., Novikov A.V. 2016. Direct numerical simulation of laminar–turbulent flow over a flat plate at hypersonic flow speeds," *Computational Mathematics and Mathematical Physics*, 56(6), pp. 1048-1064.

[4] Novikov A., Egorov I., Fedorov A. 2016. Direct Numerical Simulation of Wave Packets in Hypersonic Compression-Corner Flow. *AIAA Journal,* 54(7), pp. 2034-2050.

[5] Novikov A., Egorov I. 2016. Direct Numerical Simulations of Transitional Boundary Layer over a Flat Plate in Hypersonic Free-Stream . *AIAA Paper* 2016-3952. P.1−20.

[6] Ducros F. et.al. 1999. Large-Eddy Simulation of the Shock / Turbulence Interation. *Journal of Computational Physics* 152, 517–549.